Appendix

A.1 Kramers–Kronig Relation for Wavenumber

Assuming that the magnetic and electric susceptibility

$$\chi_m(\omega) = \chi_m(\omega)' - j\chi_m''(\omega), \tag{A.1}$$
$$\chi_e(\omega) = \chi_e(\omega)' - j\chi_e''(\omega) \tag{A.2}$$

describe the causal response to a magnetic and electric field in the frequency domain, then $\chi'(\omega)$ and $\chi''(\omega)$ is an even and odd function, respectively, so that

$$\chi_m(-\omega) = \chi_m(\omega)^*,\ \chi_e(-\omega) = \chi_e(\omega)^*. \tag{A.3}$$

With the susceptibilities, the square of the wavenumber is

$$k^2(\omega) = k_0(\omega)^2\,[1 + \chi_m(\omega)]\,[1 + \chi_e(\omega)] \tag{A.4}$$

and hence,

$$\frac{k^2(\omega)}{k_0^2(\omega)} = 1 + \chi_m' + \chi_e' + \chi_m'\chi_e' - \chi_m''\chi_e'' - j(\chi_m'' + \chi_e'' + \chi_m'\chi_e'' + \chi_m''\chi_e'). \tag{A.5}$$

The product of two even functions (two real parts) and the product of two odd functions (two imaginary parts) yields an even function while the product of an odd and an even function (product of a real and imaginary part) yields an odd function. Hence, with (A.3), the real part in (A.5) is an even function and the imaginary part an odd function and it shows the same symmetry

$$\frac{k^2(\omega)}{k_0^2(\omega)} = \left(\frac{k^2(-\omega)}{k_0^2(-\omega)}\right)^*. \tag{A.6}$$

M. Maasch, *Tunable Microwave Metamaterial Structures*, Springer Theses,
DOI 10.1007/978-3-319-28179-7

Since (A.3) and (A.6) are a consequence of Titchmarsh's theorem [1, 2], it has to hold

$$\frac{k^2(\omega)}{k_0^2(\omega)} = 1 - \frac{j}{\pi} \fint_{-\infty}^{\infty} \frac{k^2(\Omega)/k_0^2(\Omega)}{\omega - \Omega} \mathrm{d}\Omega. \tag{A.7}$$

With the approximation

$$\sqrt{1+a} \approx 1 + \frac{a}{2} \quad \text{for } |a| \ll 1, \tag{A.8}$$

the wavenumber for small susceptibilities can be approximated by

$$k(\omega) \approx k_0(\omega) \left[1 + \frac{\chi_m(\omega)}{2}\right] \left[1 + \frac{\chi_e(\omega)}{2}\right] \tag{A.9}$$

which yields

$$\frac{k^2(\omega)}{k_0^2(\omega)} \approx 1 + \frac{\chi_m'}{2} + \frac{\chi_e'}{2} + \frac{\chi_m'\chi_e'}{4} - \frac{\chi_m''\chi_e''}{4} - j\left(\frac{\chi_m''}{2} + \frac{\chi_e''}{2} + \frac{\chi_m'\chi_e''}{4} + \frac{\chi_m''\chi_e'}{4}\right). \tag{A.10}$$

It shows the same symmetry properties for the real and imaginary part as (A.5) so that the Kramers–Kronig relation has to hold for the approximation of the refractive index:

$$\frac{k(\omega)}{k_0(\omega)} \approx 1 - \frac{j}{\pi} \fint_{-\infty}^{\infty} \frac{k(\Omega)/k_0(\Omega)}{\omega - \Omega} \mathrm{d}\Omega. \tag{A.11}$$

A.2 Relation Between Two-Port Parameters

Figure A.1 shows the port-currents and voltages as they are used for all two-port networks in this work. In the following, important relations between different matrix representations are summarized.

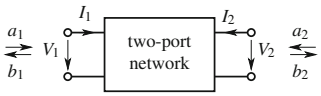

Fig. A.1 Definition of voltages and currents for a two-port network

A.2.1 Chain Parameters of a Transmission Line

The chain parameter matrix **A** with the voltages and currents as defined in Fig. A.1 for a transmission line section of the length l follows

$$\begin{pmatrix} V_1 \\ I_1 \end{pmatrix} = \mathbf{A} \cdot \begin{pmatrix} V_2 \\ -I_2 \end{pmatrix} = \begin{pmatrix} \cosh \gamma l & Z_c \sinh \gamma l \\ \frac{1}{Z_c} \sinh \gamma l & \cosh \gamma l \end{pmatrix} \cdot \begin{pmatrix} V_2 \\ -I_2 \end{pmatrix}. \tag{A.12}$$

A.2.2 Relation Between Transmission Line Parameters and Scattering Parameters

The generalized scattering parameters based on the definition of complex power waves [3–6]

$$a_i = \frac{V_i + Z_{0i} I_i}{2\sqrt{\mathrm{Re}\{Z_{0i}\}}}, \tag{A.13}$$

$$b_i = \frac{V_i - Z_{0i}^* I_i}{2\sqrt{\mathrm{Re}\{Z_{0i}\}}} \tag{A.14}$$

are calculated from the transmission line parameters by

$$S_{11} = \frac{b_1}{a_1} = \frac{(Z_{02} - Z_{01}^*)\cosh(\gamma l) + \left(Z_c - \frac{Z_{01}^* Z_{02}}{Z_c}\right)\sinh(\gamma l)}{(Z_{01} + Z_{02})\cosh(\gamma l) + \left(Z_c + \frac{Z_{01}^* Z_{02}}{Z_c}\right)\sinh(\gamma l)}, \tag{A.15}$$

$$\begin{aligned} S_{12} &= \frac{b_1}{a_2} = S_{21} = \frac{b_2}{a_1} \\ &= \frac{2\sqrt{\mathrm{Re}\{Z_{01}\}\mathrm{Re}\{Z_{02}\}}}{(Z_{01} + Z_{02})\cosh(\gamma l) + \left(Z_c + \frac{Z_{01}^* Z_{02}}{Z_c}\right)\sinh(\gamma l)}, \end{aligned} \tag{A.16}$$

$$S_{22} = \frac{b_2}{a_2} = \frac{(Z_{01} - Z_{02}^*)\cosh(\gamma l) + \left(Z_c - \frac{Z_{01} Z_{02}^*}{Z_c}\right)\sinh(\gamma l)}{(Z_{01} + Z_{02})\cosh(\gamma l) + \left(Z_c + \frac{Z_{01}^* Z_{02}}{Z_c}\right)\sinh(\gamma l)}. \tag{A.17}$$

If not noted otherwise in this work, the reference impedance Z_{0i} is purely real so that the scattering parameters based on the power wave definition and the scattering parameters based on the traveling wave definition [7, 8] are equivalent.

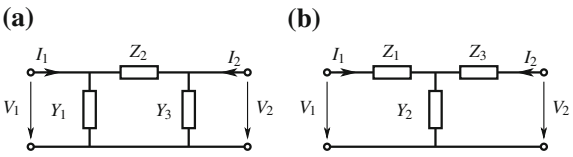

Fig. A.2 Two-port circuit: **a** in Π-configuration, **b** in T-configuration

A.2.3 Two-Port Parameters of Circuits in Π- and T-Configuration

The unit cell configurations investigated in this work can be represented by a two-port circuit in Π- or T-configuration (Fig. A.2). They yield the impedance and admittance matrix

$$\begin{pmatrix} I_1 \\ I_2 \end{pmatrix} = \mathbf{Y}_{\Pi} \cdot \begin{pmatrix} V_1 \\ V_2 \end{pmatrix} = \begin{pmatrix} Y_1 + 1/Z_2 & -1/Z_2 \\ -1/Z_2 & 1/Z_2 + Y_3 \end{pmatrix} \cdot \begin{pmatrix} V_1 \\ V_2 \end{pmatrix}, \tag{A.18}$$

$$\begin{pmatrix} V_1 \\ V_2 \end{pmatrix} = \mathbf{Z}_{\mathrm{T}} \cdot \begin{pmatrix} I_1 \\ I_2 \end{pmatrix} = \begin{pmatrix} Z_1 + 1/Y_2 & 1/Y_2 \\ 1/Y_2 & 1/Y_2 + Z_3 \end{pmatrix} \cdot \begin{pmatrix} I_1 \\ I_2 \end{pmatrix}. \tag{A.19}$$

and the chain parameter matrices

$$\mathbf{A}_{\Pi} = \begin{pmatrix} 1 + Z_2 Y_3 & Z_2 \\ -(Y_1 + Y_1 Z_2 Y_3) & 1 + Y_1 Z_2 \end{pmatrix}, \tag{A.20}$$

$$\mathbf{A}_{\mathrm{T}} = \begin{pmatrix} 1 + Z_1 Y_2 & Z_1 + Z_1 Y_2 Z_3 \\ Y_2 & 1 + Y_2 Z_3 \end{pmatrix}. \tag{A.21}$$

A.2.4 Two-Port Representation of a Transformer

A magnetic coupling between two inductors can be represented by the transformer with the coupling factor S in Fig. A.3a. The T-configuration of the transformer in Fig. A.3b takes the mutual inductance

$$M^2 = S^2 L_1 L_2 \tag{A.22}$$

into account.

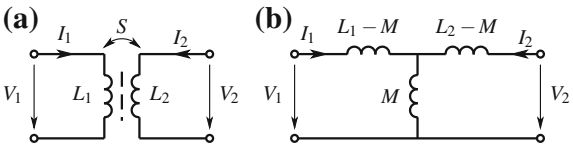

Fig. A.3 **a** Transformer with two coupled inductors. **b** T-configuration with the mutual inductance M

A.3 Photolithography Steps

In this work, different voltage tunable structures are manufactured on glass substrates. The main lithography steps, following the works [9–12], are:

- evaporation of NiCr and Au on glass substrate
- RF structure:
  - AZ4533 photo resist mask for Au plating: spin coat, softbake
  - exposure of mask for RF structure, development with AZ400K
  - hardbake (result: Fig. A.4a)
  - electroplating of Au
  - remove photo resist layer (result: Fig. A.4b)
- resistive biasing network:
  - AZ4533 photo resist mask for NiCr: spin coat, softbake
  - exposure of mask for bias lines, development with AZ400K
  - hardbake (result: Fig. A.4c)
- Selective wet etching:
  - Au etching
  - NiCr etching
  - remove photo resist layer
  - Au etching (result: Fig. A.4d)

If LC is used as tunable material, following steps are the processing and rubbing of the polyimide alignment layer and glueing of glass substrates to form the LC cavity.

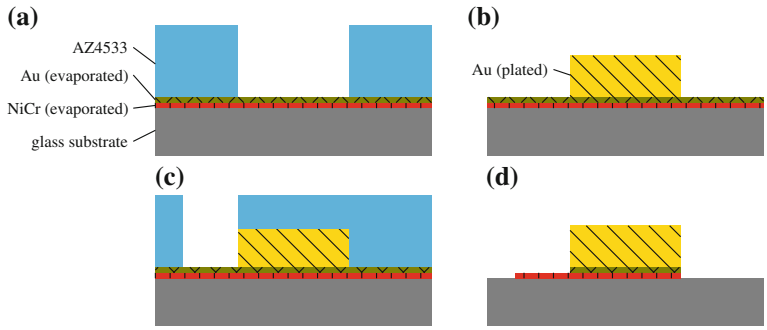

Fig. A.4 Glass substrates with Au and NiCr metallization after different manufacturing process steps: **a** photo resist for Au plating, **b** electroplated Au layer, **c** photo resist for etching of Au and NiCr, **d** final structure after wet etching

References

1. J.S. Toll, Causality and the dispersion relation: logical foundations. Phys. Rev. **104**, 1760–1770 (1956)
2. R.L. Weaver, Y.-H. Pao, Dispersion relations for linear wave propagation in homogeneous and inhomogeneous media. J. Math. Phys. **22**(9), 1909–1918 (1981)
3. D. Youla, On scattering matrices normalized to complex port numbers (1961)
4. K. Kurokawa, Power waves and the scattering matrix. IEEE Trans. Microw. Theory Tech. **13**(2), 194–202 (1965)
5. D. Frickey, Conversions between s, z, y, h, abcd, and t parameters which are valid for complex source and load impedances. IEEE Trans. Microw. Theory Tech. **42**, 205–211 (1994)
6. J. Freeman, On the interpretation of scattering parameters, Technical report, NASA Technical Reports Server, 1999
7. R.B. Marks, D.F. Williams, A general waveguide circuit theory. J. Res.-Natl. Inst. Stand. Technol. **97**, 533 (1992)
8. R.B. Marks, D.F. Williams, D. Frickey, Comments on conversions between s, z, y, h, abcd, and t parameters which are valid for complex source and load impedances [with reply]. IEEE Trans. Microw. Theory Tech. **43**(4), 914–915 (1995)
9. A. Mössinger, R. Marin, S. Müller, J. Freese, R. Jakoby, Electronically reconfigurable reflectarrays with nematic liquid crystals. Electron. Lett. **42**(1), 899–900 (2006)
10. F. Gölden, A. Gäbler, S. Müller, A. Lapanik, W. Haase, R. Jakoby, Liquid-crystal varactors with fast switching times for microwave applications. Electron. Lett. **44**(7), 480–481 (2008)
11. F. Gölden, Liquid crystal based microwave components with fast response times: material, technology, power handling capability, Ph.D. thesis, Technische Universität Darmstadt, Fachgebiet Mikrowellentechnik, June 2010
12. O.H. Karabey, Electronic beam steering and polarization agile planar antennas in liquid crystal technology, Ph.D. thesis, TU Darmstadt, Cham, 2014. Zugl. Darmstadt, Techn. Univ., Diss., 2013